




Femtosecond laser dentistry for precise and efficient cavity preparation in teeth

LUDOVIC RAPP,^{1,*}  STEVE MADDEN,¹ JULIA BRAND,^{1,2} 
LAURENCE J. WALSH,^{3,4} HEIKO SPALLEK,⁵ OMAR ZUAITER,⁴ ALAA HABEB,⁴ TIMOTHY R. HIRST,⁴ AND ANDREI V. RODE¹

¹*Department of Quantum Science and Technology, Research School of Physics, Australian National University, Canberra, ACT 2600, Australia*

²*Centre for Creative and Cultural Research, Faculty of Art and Design, University of Canberra, ACT 2617, Australia*

³*The University of Queensland School of Dentistry QLD 4006, Australia*

⁴*Dentroid (Emudent Technologies Pty Ltd), Canberra ACT 2601, Australia*

⁵*The University of Sydney School of Dentistry, Faculty of Medicine and Health, NSW 2010, Australia*

*ludovic.rapp@anu.edu.au

Abstract: High fluence focused femtosecond laser pulses were used to perform fast, high precision and minimally damaging cavity cutting of teeth at room temperature without using any irrigation or cooling system. The optimal ablation rates were established for both enamel and dentin, and the surfaces were assessed with optical and scanning electron microscopy, Raman spectroscopy and optical profilometry. No chemical change in the composition of enamel and dentin was observed. We explored temperature variations inside the dental pulp during the laser procedure and showed the maximum increase was 5.5°C, within the acceptable limit of temperature increase during conventional dental treatments.

© 2022 Optica Publishing Group under the terms of the [Optica Open Access Publishing Agreement](#)

1. Introduction

Dentistry today is subject to a rapid accelerating demand driven by the high prevalence of oral diseases due, in part, to sugary diets [1], changes in body image that call for cosmetic procedures [2,3], demographic trends of a dentulous aging population [4], emerging economies, and increased awareness. Untreated dental caries, severe periodontitis, and tooth loss are among the ten most prevalent conditions, globally affecting more than 3.5 billion people in 2017 [5].

In the dental office, the removal of hard tissue involves two methods: (1) the traditional grinding by rotating drills that started at slow speeds about a hundred years ago, inflicting severe pain due to vibrations, and that now rotate at speeds of up to 400,000 rpm, reducing vibrations and the associated annoyance factor, but requiring constant water cooling to avoid overheating the living tissues; and (2) newer ablation techniques such as by using erbium lasers (Er:YAG and Er,Cr:YSGG). Both methods generate mechanical and thermal stress that can lead to the formation of micro-cracks in the enamel on several tens of microns. These are potential initiation sites for new bacterial and chemical attacks leading to carious lesions and have to be avoided for the long-term success of the dental treatment. While erbium lasers with a water mist spray reduce thermal effects considerably, they cannot compete with the speed or quality of cutting using high-speed dental drills [6–8]. Moreover, the precision of cutting using these lasers is limited by the large size of the individual crater that each laser pulse creates, as well as micromovements of the handpiece held by the dentist, and movements of the patient’s body, head, and lower jaw. These small movements mean that the engineering approach of “fit and finish” is difficult to achieve, even when the dentist views their work through magnifying loupes or an operating microscope.

Microsecond pulsed Erbium lasers have been used to prepare teeth for restorative procedures since the 1990s. They rely on a photomechanical process, whereby the absorption of laser energy in water and hydroxyl groups in the material creates explosions of steam which then detach particles from the tooth [8]. The explosion is accompanied by shock waves which propagate through the tooth and which can themselves cause microscopic cracks in the tooth structure at the edges of individual craters. Erbium lasers all require a water mist spray to operate effectively, and to prevent burning, carbonization and thermal stress to the dental pulp [7,8]. An excessively high rate of water flow interferes with the laser ablation action by attenuating the beam, while an insufficient film of water will lead to burning and carbonization of the tooth, with cracking and thermal stress.

Using ultrashort pulses mitigates problems caused by thermo-mechanical actions. With ultrashort pulses, the instantaneous peak power is very high, which means that it is not necessary to use a laser wavelength strongly absorbed in either water or the mineral component of tooth structure, i.e., hydroxyapatite. The ability to control the ablation process much more precisely by altering the pulse energy and the scanning pattern allows the tooth to be machined to give a smooth surface without inducing heat within the tooth itself. Accurate control of the extent to which pulses overlap requires going beyond hand-held handpieces. In the past few years, femtosecond lasers have been used widely in medical areas such as vision correction surgery (such as LASIK), cataract surgery, ear surgery, and tattoo removal. For restorative dentistry, such lasers can overcome the drawbacks of traditional treatment methods [9]. Since the mid-1990s, a growing number of studies have demonstrated that femtosecond laser ablation represents the first viable alternative to high-speed dental drills operated by air turbines or electric micromotors [10–21]. The femtosecond laser ‘drill’ is much quieter and causes little to no direct pain during its operation. Studies of femtosecond laser ablation of enamel and dentin using scanning electron microscopy have confirmed crack-free cavities in teeth, with a processing precision of 10 μm [22,23]. This exceeds the precision that handheld high-speed drills can achieve and is far more precise than ablation by erbium or other middle- or far-infrared lasers.

With the recent emergence of powerful femtosecond lasers generating high peak energy and high repetition rate, it is now possible to envisage a system using such a laser that could compete with high-speed dental drills in terms of the rate of removal of tooth structure, and with outstanding precision. Such devices could, unlike existing erbium lasers, ablate a wide range of filling materials in teeth. In this paper, we investigated the ablation performance of a high fluence and high scanning rate femtosecond laser for application in dentistry. We determined the ablation threshold of the enamel and the dentin constituting the tooth, investigated the optimum conditions by optical profilometry, optical and scanning electron microscopy, performed Raman characterization of the processed tooth structure, and monitored and analysed thermal loads into the tooth body during the laser process using a micro-thermocouple embedded into the dental pulp chamber. This study, for the first time, demonstrates comprehensively how femtosecond lasers can revolutionize dentistry by providing an efficient, versatile, pain-free, and fast way to remove decayed and healthy dentin and enamel as well as various restorative materials.

2. Experimental details

2.1. Teeth

Intact health human permanent teeth, collected with institutional human ethics approval, were used to study the effects of the femtosecond laser. These teeth had been collected as part of a previous study on laser processing using Er:YAG lasers [7]. They were selected from a collection of extracted teeth removed for orthodontic purposes and were used intact or were sectioned horizontally with a diamond saw (Buehler, Lake Bluff, IL, USA). Remnants of dental pulp tissue were removed. After preparation, the teeth were sterilized by gamma irradiation (25 kGray, Steritech, Narangba, Qld, Australia) and stored in a dry state. They were rehydrated with distilled

water for 24hr before laser processing so that their water content was restored to the normal fully hydrated state.

2.2. Experimental setup

The femtosecond laser processing experiments on the enamel and the dentin of the teeth were performed with a Carbide 40W femtosecond laser (CB3-40W from Light Conversion, Lithuania). The laser wavelength was 1029 nm (fundamental) and the pulse duration was set to 275 fs. The repetition rate was 100 kHz and the pulse energy 400 μ J. The laser pulses were focused on the sample with a quasi-telecentric f-Theta scanning lens of 540 mm working distance (S4LFT1420/449, Sill Optics GmbH, Germany). The focal spot diameter for the raw beam was \sim 94 μ m at FWHM. The beam size was reduced to 54 μ m (FWHM) with a GBE02-C – 2X achromatic Galilean beam expander (Thor Labs Inc.).

A 10-facets polygon mirror (Precision Laser Scanning Inc., USA) and a galvanometer scanner (Cambridge Technology Inc., USA) were used to scan the beam across the teeth in the single-pulse scanning regime, with well separated laser spots on the target surface. The fast (vertical) scan in the raster pattern was formed by the polygon scanner rotation at 1,000 rpm providing a beam velocity at the point of focus of \sim 86 m/s. The steps between each polygon scanner line were provided by the galvo scanner at a velocity at the point of focus of \sim 20 m/s, with a step of 5 μ m on the surface.

The laser fluence was varied by attenuating the laser power. In-house written LabView software controlled the laser beam scanning characteristics, such as scanning speed, inter-shot, inter-scan line distance, and two-dimensional (2D) scanning pattern design. An extraction system (Kemper) with an exhaust capacity of 950 m³/h has been used to collect all ablated materials during the experiments. All experiments were undertaken in ambient air at room temperature. A schematic of the experimental setup is presented in Fig. 1.

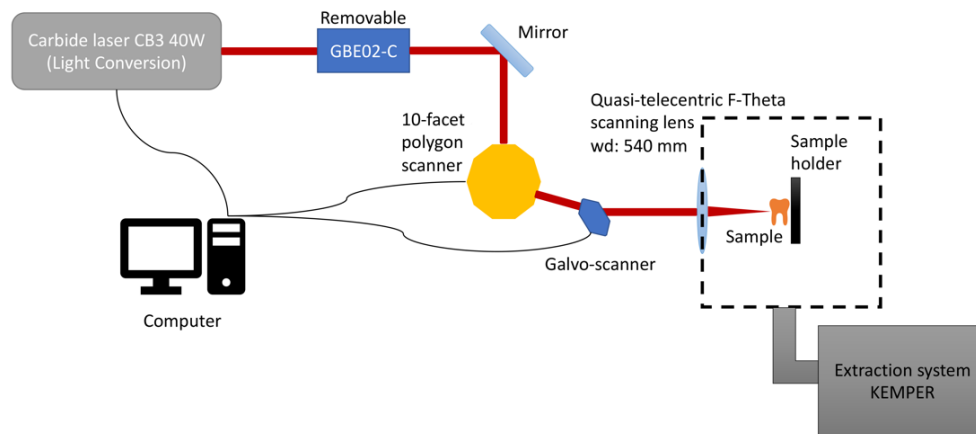


Fig. 1. Schematic of the experimental setup.

2.3. Characterization methods

The ablated surfaces were observed with an optical microscope. Surface texture, roughness and depth of the ablated surface were recorded by using an optical profiler (Veeco Wyko NT9100, Bruker, USA) with a 5 \times and 20 \times objective and a 0.55 \times field-of-view multiplier. The vertical scanning interferometry (VSI) mode was used.

Surface features were assessed for structural changes induced by the laser by scanning electron microscopy at magnifications up to 5,000 \times using a Zeiss UltraPlus FESEM, with an accelerating

voltage of 10 kV and a sample working distance of 2–5 mm. The samples were sputter coated with carbon prior to examination by scanning electron microscopy.

Raman micro-spectroscopy using a Renishaw InVia Reflex Raman spectrometer was used to investigate the possible chemical changes in the tooth structures before and after the laser treatments. Spectra were obtained with a 785 nm near infrared diode laser focused on the tooth using a 20× lens (with a 1.15 mm working distance). A grating with 1200 lines/mm was used for all measurements, and the spectra were collected on a Peltier-cooled CCD detector. Three scans with an acquisition time of 20s were undertaken over a spectral range of 300-1800 cm^{-1} for dentin and enamel, using a laser power of 3.8 mW. Calibration used the 520.7 cm^{-1} peak of a silicon reference. The raw spectra were baseline-corrected with BSpline software interpolation, then smoothed with the Savitzky-Golay filter of polynomial order 3 and 24 points, then normalized to the 959 cm^{-1} peak and curve-fitted with Gaussian peak profiles to precisely determine the peak positions.

2.4. Temperature measurement details

Temperature changes during laser processing were recorded by inserting a 0.5 mm diameter miniature bead thermocouple inside the dental pulp chamber of each tooth. The bead was covered with heat conductive heatsink compound before being fixed to ensure that heat transfer occurred from the dentin. The position of the thermocouple was against the dentin directly opposite the point of laser processing where the dentin thickness was least, to measure the maximal thermal changes [7]. Data during laser processing were collected using a data logger (Lascar), and the maximum temperature change was calculated. The experiments were repeated on several teeth for time durations ranging from 1 min of laser treatment to 40 min.

3. Results and discussion

3.1. Femtosecond laser processing of tooth-ablation threshold and ablation rate

The ablation threshold and the ablation rate were investigated for both the enamel and the dentin of healthy human teeth cut transversally with a diamond saw. Using the femtosecond laser, grooves were prepared in enamel and in dentin using different fluences, with the number of pulses and the overlap of the pulses adjusted to keep the total energy per pulse constant.

The ablation depth per shot was plotted as a function of the fluence for enamel and dentin. These data are presented in Fig. 2(a) together with their respective ablation rates. These results demonstrate that enamel and dentin are ablated at different rates. Enamel was more difficult to ablate, with an ablation threshold of $1.1 \pm 0.1 \text{ J/cm}^2$. Dentin was ablated more easily, with a lower ablation threshold of $0.6 \pm 0.1 \text{ J/cm}^2$. The maximum ablation rate for enamel occurred at 12 J/cm^2 with $27.2 \text{ mm}^3/\text{min}$ ($0.45 \text{ mm}^3/\text{s}$), while the corresponding rate for dentin was $39.0 \text{ mm}^3/\text{min}$ ($0.65 \text{ mm}^3/\text{s}$).

It is important to note here that the maximum ablation rate did not correspond necessarily to the optimum ablation regime. Figure 2(b) and 2(c) present the data for the ablation efficiency of enamel and dentin. Enamel had an optimum ablation efficiency of $0.93 \text{ mm}^3/\text{min/W}$ ($0.0155 \pm 0.0005 \text{ mm}^3/\text{J}$) at 6.11 J/cm^2 . Ablation of dentin was far more efficient, at $2.20 \text{ mm}^3/\text{min/W}$ ($0.0366 \pm 0.0005 \text{ mm}^3/\text{J}$) at an energy density of only 2.45 J/cm^2 . Figure 2(b) shows the ablation efficiency when the full 40 W of laser power was used, with the rates being $37.2 \text{ mm}^3/\text{min}$ for enamel, and $88.0 \text{ mm}^3/\text{min}$ for dentin. The ablation rate and efficiency decreased with increasing laser fluence. These results may be explained by the fact that the optical breakdown, which is a highly non-linear process, happens earlier during the pulse, and therefore a larger part of the laser energy goes into increasing the laser-produced plasma temperature instead of delivering the energy to the solid surface.

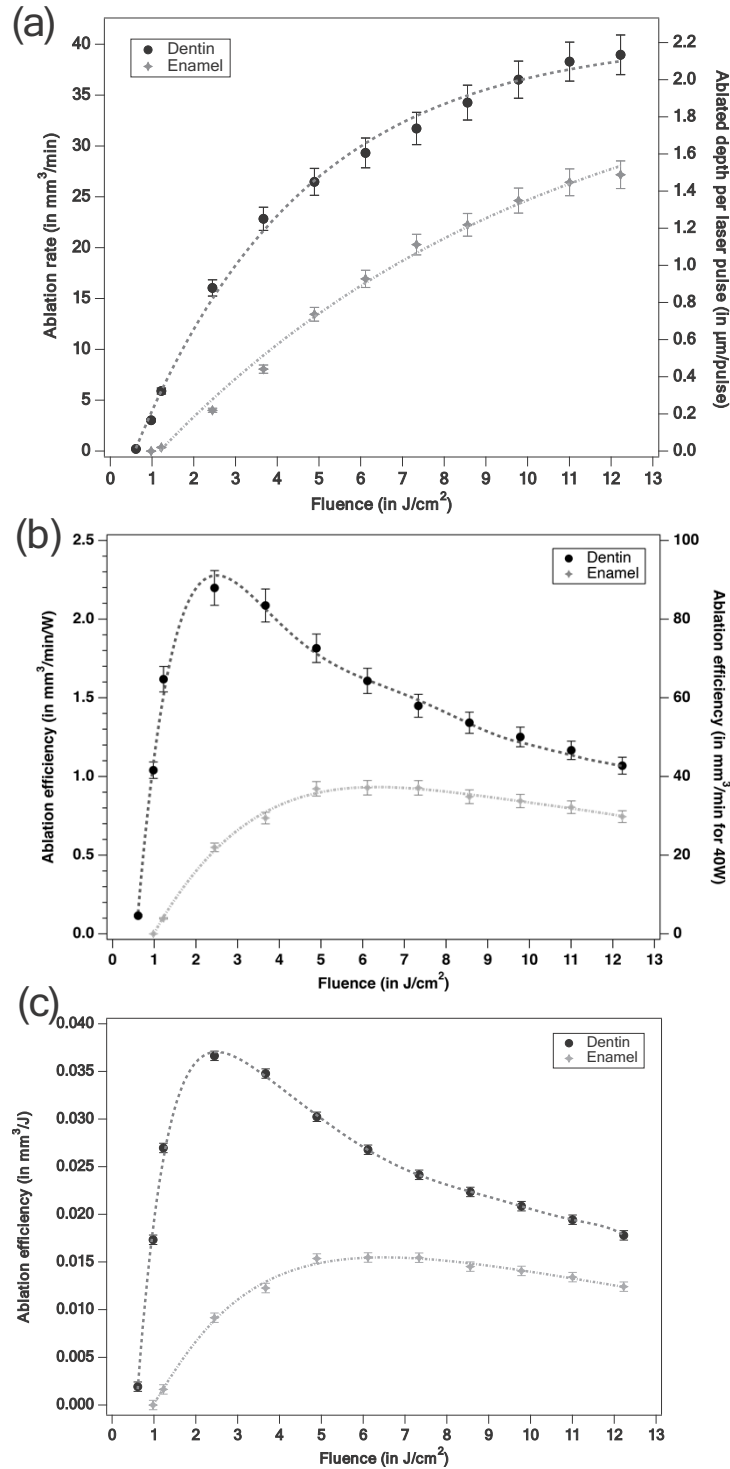


Fig. 2. Femtosecond laser processing of enamel and dentin: (a) ablation rate and ablated depth per laser pulse; (b) ablation efficiencies; (c) relationship between laser fluence and ablation efficiency.

With these parameters now established, it was then possible to prepare precise and sharp parallel grooves in enamel and in dentin at high scanning rates. Figure 3 presents optical microscope images of grooves and cavities made using the optimum laser regime in different parts of teeth. Cavities were cut in the outer enamel of the buccal aspect of premolar teeth, in its center and on the edges or line angles (Fig. 3(a)). Additional molar teeth that had been sectioned horizontally were used for preparing grooves and cavities in enamel and extending across both dentin and enamel (Fig. 3(b) and (c)). A further molar tooth was sliced and laser-processed entirely on half of the surface (Fig. 3(d)), coming from an occlusal direction in the same manner as would be done when a laser is applied in clinical practice.

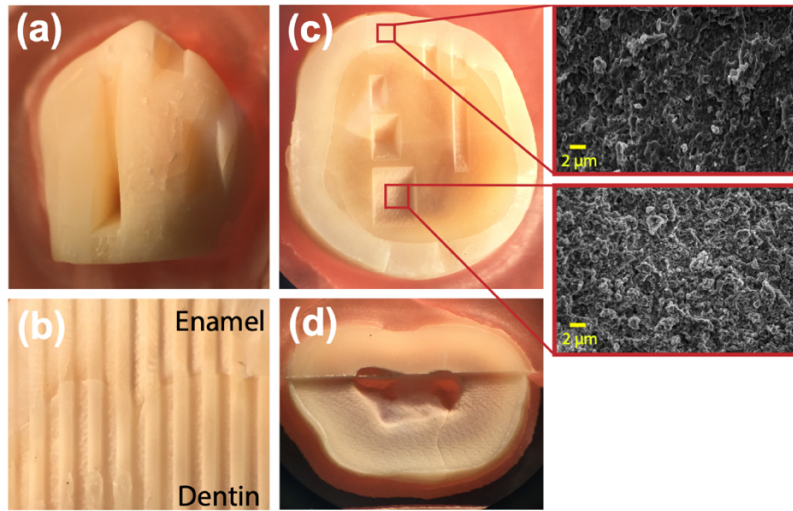


Fig. 3. Optical microscopy and scanning electron microscopy images of laser processed teeth showing prepared cavities in enamel and dentin: (a) prepared grooves in enamel; (b) horizontally sliced tooth with grooves prepared in both enamel and dentin; (c) horizontally sliced tooth with cavities, insets show SEM views of the cavity floor for processed enamel and dentin; (d) sliced tooth with horizontal surface processed using the laser.

SEM characterization was performed on the bottoms of the prepared cavities inside of the tooth to inspect the processed surface topographies. Microscale roughness can be observed in the dentin, where some open tubules are present. In the enamel, a globular pattern can be seen, with contour variations in the range of 1 to 10 μm approximately. All irregularities on the cavity floors and walls in both the enamel and the dentin are in the micron size range, which means that at the macroscopic level, the cavity walls and floors were smooth. Overall, the surfaces are clean with no cracking nor photothermally induced damage.

Figure 4 presents optical microscope images of grooves laser-processed at 6.11 J/cm² in enamel and in dentin, together with the corresponding surface profilogram measurements. Precise cuts in both enamel and in dentin with sharp edges were observed. The average roughness of the bottom of the groove in enamel was $7 \pm 1 \mu\text{m}$ and $11 \pm 2 \mu\text{m}$ in dentin. It was noted that for the same fluence and the same number of pulses, the grooves in dentin were deeper, as expected from the ablation efficiency analysis.

3.2. Investigation of possible chemical changes by Raman micro-spectroscopy

The laser treated and untreated surfaces of several teeth were investigated and compared using Raman micro-spectroscopy. Figure 5 presents the spectra of laser-processed and unprocessed enamel (a) and dentin (b) without curve fitting for clarity. The spectra of enamel and dentin

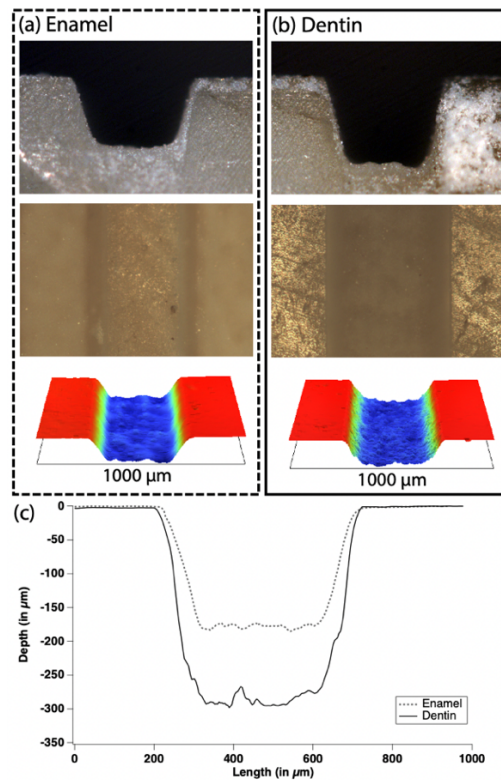


Fig. 4. Femtosecond laser processed grooves prepared at 6.11 J/cm^2 in (a) enamel and (b) dentin. Upper panels show optical microscope images of the prepared cavities in cross-section and viewed from the top, together with the corresponding 3D surface profilograms; (c) surface profilograms of typical prepared grooves in enamel (dotted line) and dentin (continuous line).

are typical of carbonated hydroxyapatite. The spectrum of enamel (Fig. 5(a)) contains seven peaks, with the main feature centered at $959.96 \pm 0.02 \text{ cm}^{-1}$. This peak was attributed to the symmetric stretching vibration of the phosphate PO_4 units in the apatite. The phosphate units exhibit three other vibrations [24]: the symmetric bending mode recorded at $427.5 \pm 0.4 \text{ cm}^{-1}$, the antisymmetric bending mode at $584.72 \pm 0.4 \text{ cm}^{-1}$ and the antisymmetric stretching mode at $1041.4 \pm 2.1 \text{ cm}^{-1}$. Additional peaks were recorded at $1070.3 \pm 0.8 \text{ cm}^{-1}$, attributed to the symmetric stretching of carbonate, which can overlap with the antisymmetric stretching of PO_4 [25]. Another peak at $614.3 \pm 0.7 \text{ cm}^{-1}$ was attributed to the antisymmetric bending of PO_4 and at $444.5 \pm 1.6 \text{ cm}^{-1}$ attributed to the symmetric bending of PO_4 [26].

The spectra of dentin (Fig. 5(b)) showed the features of hydroxyapatite previously discussed. The symmetric bending mode of phosphate was recorded at $434.83 \pm 0.33 \text{ cm}^{-1}$, and the antisymmetric stretching mode of phosphate was visible at $1024.55 \pm 1.63 \text{ cm}^{-1}$. Additional peaks characteristic of the organic content of dentin were observed at $1240.7 \pm 0.1 \text{ cm}^{-1}$ and attributed to a mix of C-N stretching vibration and N-H bending vibration of amide III, at $1455.44 \pm 0.70 \text{ cm}^{-1}$ characteristic to CH_2 wagging, and at $1665.92 \pm 0.75 \text{ cm}^{-1}$ attributed to the in-plane stretching of carbonyl from peptide bonds in amide I [27]. The flat area between the 1240 and 1450 cm^{-1} is an artefact due to the baseline correction and smoothing.

Overall, the obtained Raman spectra revealed no damage nor chemical changes induced to the mineral and organic phase of the tooth after laser processing. As can be seen in Fig. 5, the

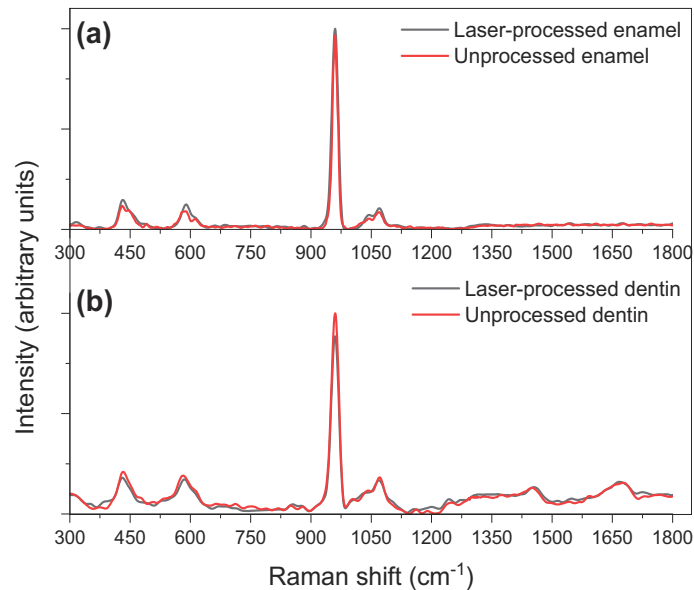


Fig. 5. Raman spectra of (a) femtosecond laser-processed and unprocessed enamel; (b) femtosecond laser-processed and unprocessed dentin.

spectra of unprocessed and laser-processed enamel overlap precisely when they are overlaid. The paired spectra do not show frequency shifts or modification of the shape of the peaks such as broadening, which usually indicate loss of crystallinity and would suggest potential damage induced to the tooth. Similarly, for dentin, the unprocessed and laser-processed spectra when overlaid did not exhibit any differences.

3.3. Temperature measurements during fs laser processing

For laser procedures on teeth, elevations in temperature of the dental pulp should not exceed a tolerance level defined historically as a temperature rise of 5.5 degrees sustained for more than 10 sec. This value is derived from a study undertaken in 1965 on monkeys, whose teeth were stressed by applying a heat source. The dental pulp tissues were then assessed by histology after 2, 7, 14, 56, and 91 days. Once the temperature of the dental pulp increased by 5.5°C from the prolonged application of the heat source for more than 10 sec, soft tissue irritation and inflammation (pulpitis) occurred. In some 15% of cases, this led to dental pulp necrosis [28].

Despite these findings, a later in vivo study undertaken on human in 1997 showed that transient temperature increases of 8.9 - 14.7°C could be tolerated without adverse outcomes since they did not cause permanent damage to the dental pulp at the histological level [29]. In this study, the thermal stimulus was maintained for about 30 seconds after the patient reported that the stimulus had become painful. Hence, the speed, the duration, and the temperature of the thermal stimulus are the parameters that determine if significant injury occurs to the dental pulp [30,31].

Accurate measurement of temperature changes at the level of the dental pulp during dental procedures can be done using miniature thermocouples [7,30], especially when intact whole teeth are used, and they are maintained in a water bath at body temperature to ensure more realistic thermodynamics than an isolated tooth. The dissipation of heat within a tooth on the benchtop will miss the cooling effects of pulpal blood flow, as well as the dissipation of heat by blood circulation through the adjacent periodontal ligament and alveolar bone [30]. Consequently,

assessments of temperature change on the bench must be interpreted with great caution as they typically will overestimate the extent of change versus what occurs *in vivo* [30].

Unlike the situation with a high-speed dental drill and an erbium laser, in the present study, no accompanying water spray was used during laser treatment, and no other special efforts, such as the application of compressed air to the target, were made. Bearing in mind these caveats, the results of the present study for temperature changes inside teeth during laser processing are noteworthy. A typical experimental run is shown in Fig. 6, which presents data for changes in temperature during a 6.5 min laser procedure, when the room temperature was stable at 21.5°C. It is instructive to note here that the tooth was effectively thermally isolated, and we used a polygon scanner to scan the laser beam across the tooth in the single pulse per spot ablation/scanning regime. For a square of $2 \times 2 \text{ mm}^2$ (Fig. 6(c)), the tooth is ablated with three 140 μJ pulses (at 133 kHz repetition rate) per polygon scanning line taking a time of 30 μs per line and the tooth then cools down for $\sim 6.57 \text{ ms}$ before the next scanning line arrives.

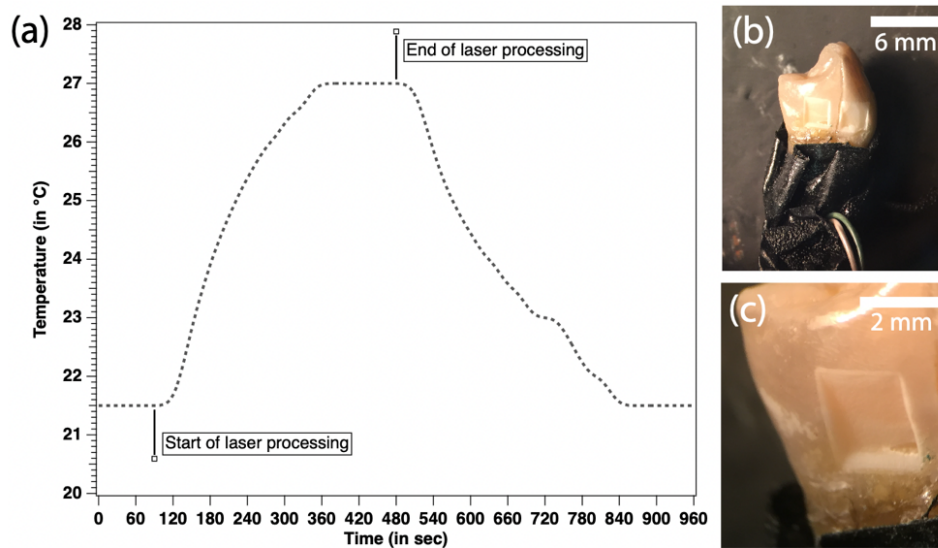


Fig. 6. (a) Recorded temperature changes during femtosecond laser processing of a mandibular first premolar tooth using a thermocouple inserted inside the dental pulp chamber (nerve canal) with (b) the corresponding laser processed tooth and (c) magnified view of one cavity.

The temperature rise plateaued at 5.5 °C to reach a maximum temperature of 27.0°C at 3 min and 25 sec (± 10 sec) after starting the laser procedure. Hence, in the worst-case scenario with no external air or conductive cooling, the internal temperature of the tooth increased by 5.5°C, reaching the threshold limit for an acceptable change. After the end of the laser procedure, free cooling of the tooth back to the baseline of room temperature took 5 min 46 sec (± 10 sec).

Further runs were undertaken using longer laser treatment times and different samples. Regardless of these changes, the maximum temperature recorded was the same for all investigated teeth and for all longer processing times. On the other hand, when shorter laser processing times were used, temperature changes were reduced. All laser procedures shorter than 1 min only increased the internal temperature of the tooth by 1.3°C. In contrast, for dental drills, a rapid rise in temperature occurs at the level of the dental pulp [30]. This rise occurs even faster when no water spray is used. One study has reported a maximum dental pulp temperature rise of 24.7°C for teeth prepared using a dental drill without water spray. The same study also noted that when a

low-speed dental drill is used, the threshold of 5.5°C is passed only 20 sec after the bur contacts the tooth surface it is cutting [32].

The temperature experiments with the femtosecond laser treatment were then reproduced with a continuous flow of compressed air directed onto the overall target area. In this situation, no change of pulpal temperature was recorded during the full laser process. It can be concluded that for femtosecond laser processing, this simple measure eliminates concerns about temperature changes, regardless of how long the laser is operating [33]. The maximum temperature was reached after ~ 3.5 min, which is a relatively slow rate of temperature rise for the femtosecond laser treatment.

3.4. Cavity preparation

Figure 7(a) presents an occlusal (top-view) view and proximal (side-view) of a mandibular left lower second premolar tooth. A cavity was prepared by ablating the enamel from the top surface of the tooth until reaching 4.5 mm in depth inside the tooth structure including the dentin, average depth of 3.25 mm. The laser process was performed at the optimal ablation regime for enamel, 6.11 J/cm^2 . The ablated area was set to $8.0 \times 4.5 \text{ mm}^2$ with an opening on one side to get a clear view of the processed regions and assess the cut quality. Figure 7(b) shows the ablated tooth from the top and three side-view images with a schematic of the processed area. Exposed dentin is clearly seen in the center of the tooth. Sharp and straight walls are observed demonstrating the precision of the cuts. The floor of the cavity is smooth, and the irregularities are due to the laser following the natural anatomy of the tooth as required when performing dental surgery. However, if required, a flat floor can be obtained by selectively ablating the higher regions until a homogeneous and flat bottom is obtained. This femtosecond laser prepared cavity demonstrates that femtosecond laser dentistry is a viable alternative to existing rotary tooth drilling technique.

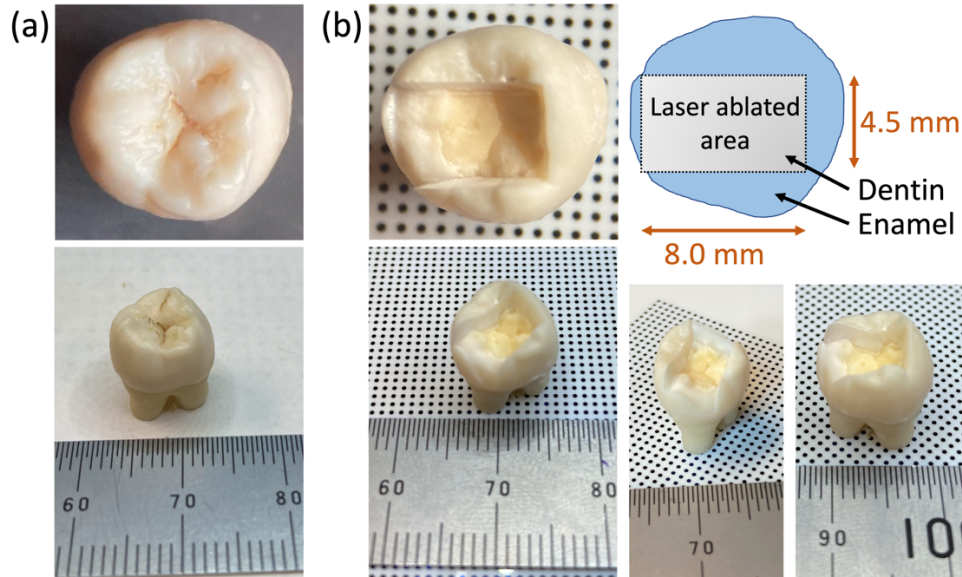


Fig. 7. (a) Occlusal view of a mandibular left second premolar tooth (b) cavity prepared in the tooth with schematic of the femtosecond laser ablated area, the ablated area is $8.0 \times 4.5 \text{ mm}^2$, and the depth is 4.5 mm with an average of ~ 3.25 mm.

4. Conclusion

This paper demonstrates that femtosecond laser pulses can quickly ablate sharp and precise grooves and cavities within the enamel and dentin of sound human permanent teeth, without significant changes occurring in terms of temperature change inside the tooth, or in terms of the chemical composition of the treated surfaces. More importantly, the laser treatments were being undertaken without using water sprays to cool the tooth. Maintaining any periods of femtosecond laser tooth processing shorter than 1 min will keep changes in dental pulp temperature below 1.3°C for a thermally isolated tooth (and likely will be much lower for a tooth *in vivo*), while using compressed air during laser processing will mitigate any thermal changes. Raman spectroscopy revealed that in the floor of the prepared grooves and cavities, there had been no change in the molecular bonds for mineral and organic constituents of tooth structure.

As current industrial femtosecond lasers deliver up to a million pulses per second, high scanning rates can be used. Only a very small amount of material is removed with each laser pulse. Consequently, the surfaces are smooth at the macroscopic level and have a roughness of less than 10 µm. For enamel, the hardest human tissue, the ablation threshold was 1.1 ± 0.1 J/cm², and the highest efficiency in the optimal volume ablation regime was found to be of 0.93 mm³/min/W for a fluence of 6.11 J/cm². For dentin, the ablation threshold was lower, at 0.6 ± 0.1 J/cm², and the highest ablation efficiency was more than twice the enamel one with 2.20 mm³/min/W for a fluence of 2.45 J/cm². Using the full 40W power of femtosecond laser, the maximum ablation rate was 37.2 mm³/min for enamel and 88.0 mm³/min for dentin.

Further studies will explore femtosecond laser treatments of unhealthy tooth structure modified by the presence of dental caries, and the processing of dental restorative materials. With the recent commercial availability of powerful femtosecond lasers, devices based on them should be able to outperform conventional dental high-speed drills. Such an approach would be a major paradigm shift, as it could open up new perspectives for precise and conservative dental treatment, instead of focusing on merely increasing the speed of rotating drills as has been the case for the recent decades. We envisage that harnessing the synergy of the femtosecond laser systems and the recent advanced in robotics will allow developing a miniaturized intraoral dental robotic device that clamps onto teeth and is remotely controlled, to perform efficient, fast, and ultra-precise laser treatments of teeth and dental restorative materials. It will free the dentists from repetitive manual operations, physical strain and proximity to the patient's oro-pharyngeal area that potentially contains infectious agents. The technology will provide patients with high-accuracy, minimally invasive and pain-free treatments, give practical solutions to dentistry's enduring issues, and improve the overall access to oral healthcare for communities at large.

Funding. Dentroid (Emudent Technologies Pty Ltd).

Acknowledgements. The authors thank Sepanta Hosseinpour for sectioning the teeth. The authors acknowledge the facilities, and the scientific and technical assistance, of the Australian Microscopy & Microanalysis Research Facility at the Centre of Advanced Microscopy, at the Australian National University. The authors acknowledge the Department of Electronic Materials Engineering (EME) of the Research School of Physics at the Australian National University for the access to the Raman spectrometer.

Author Contributions L.R., S.M., A.V.R., O.Z. A.H. and T.R.H. initiated the project. O.Z. A.H. and T.R.H. funded and administered the project. L.R., S.M. and A.V.R. designed and constructed the experimental setup. L.R. planned and performed the experiments. L.R. performed scanning electron microscopy, and images were evaluated by L.J.W. J.B. performed the Raman spectrometry and analysis. L.R., S.M. and A.V.R. analyzed the data. L.R., S.M., A.V.R., L.J.W. and H.S. analyzed the results. O.Z. A.H. and T.R.H. verified the experimental protocol and the test reports. L.R., S.M., A.V.R., H.S. and L.J.W. wrote the manuscript, with input from all authors. All authors discussed the results and contributed to manuscript preparation.

Disclosures. Authors O.Z., A.H., T.H. and L.J.W. are affiliated with or employed by Dentroid (Emudent Technologies Pty Ltd). All other authors declare no competing financial interests.

Data availability. Data underlying the results presented in this paper are not publicly available at this time but may be obtained from the authors upon reasonable request.

References

1. M. A. Peres, L. M. D. Macpherson, R. J. Weyant, B. Daly, R. Venturelli, M. R. Mathur, S. Listl, R. Keller Celeste, C. C. Guarnizo-Herreño, C. Kearns, H. Benzian, P. Allison, and R. G. Watt, "Oral diseases: a global public health challenge," *Lancet* **394**, 394 (2019).
2. A. C. L. Holden, "Consumed by prestige: the mouth, consumerism and the dental profession," *Med Health Care and Philos* **23**(2), 261–268 (2020).
3. A. C. L. Holden, "Cosmetic dentistry: A socioethical evaluation," *Bioethics* **32**(9), 602–610 (2018).
4. Australian Institute of Health and Welfare, "Oral health and dental care in Australia", Web report, (2022).
5. S. Listl, C. Quiñonez, and M. Vujicic, "Including oral diseases and conditions in universal health coverage," *Bull. World Health Organ.* **99**(6), 407 (2021).
6. L. J. Walsh, "The current status of laser applications in dentistry," *Aust. Dent. J.* **48**(3), 146–155 (2003).
7. O. B. Al-Batayneh, W. K. Seow, and L. J. Walsh, "Assessment of Er:YAG laser for cavity preparation in primary and permanent teeth: a scanning electron microscopic and thermographic study," *Pediatr. Dent.* **36**(3), 90–94 (2014).
8. G. J. Mount, L. J. Walsh, and A. M. Brostek, "Instruments used in cavity preparation," Chapter 8 in G.J. Mount, W. R. Hume, H. C. Ngo, and M. S. Wolff, (eds), *Preservation and Restoration of Tooth Structure*, 3rd edn. (John Wiley, 2016), pp. 117–138.
9. S. H. Chung and E. Mazur, "Surgical applications of femtosecond lasers," *J. Biophotonics* **2**(10), 557–572 (2009).
10. M.H. Niemz, *Laser-Tissue Interactions: Fundamentals and Applications* (Springer-Verlag, Berlin, 2004).
11. E. G. Gamaly, A. V. Rode, B. Luther-Davies, and V. T. Tikhonchuk, "Ablation of solids by femtosecond lasers: ablation mechanism and ablation thresholds for metals and dielectrics," *Phys. Plasmas* **9**(3), 949–957 (2002).
12. P. Weigl, A. Kasenbacher, and K. Werelius, in *Femtosecond Technology for Technical and Medical Applications* (Springer-Verlag Berlin, 2004), pp. 167.
13. R. F. Z. Lizarelli, M. M. Costa, E. Carvahlo-Filho, F. D. Nunes, and V. S. Bagnato, "Selective ablation of dental enamel and dentin using femtosecond laser pulses," *Laser Phys. Lett.* **5**(1), 1–8 (2008).
14. A. Daskalova, S. Bashir, and W. Husinsky, "Morphology of ablation craters generated by ultra-short laser pulses in dentin surfaces: AFM and ESEM evaluation," *Appl. Surf. Sci.* **257**(3), 1119–1124 (2010).
15. S. Alves, V. Oliveira, and R. Vilar, "Femtosecond laser ablation of dentin," *J. Phys. D: Appl. Phys.* **45**(24), 245401 (2012).
16. M. C. L. Luengo, M. Portillo, J. M. Sánchez, M. Peix, P. Moreno, A. Garcia, J. Montero, and A. Albaladejo, "Evaluation of micromorphological changes in tooth enamel after mechanical and ultrafast laser preparation of surface cavities," *Lasers Med Sci* **28**(1), 267–273 (2013).
17. H. Chen, J. Liu, H. Li, W. Ge, Y. Sun, Y. Wang, and P. Lu, "Femtosecond laser ablation of dentin and enamel: relationship between laser fluence and ablation efficiency," *J. Biomed. Opt.* **20**(2), 028004 (2015).
18. Q. Le, C. Bertrand, and R. Vilar, "Structural modifications induced in dentin by femtosecond laser," *J. Biomed. Opt.* **21**(12), 125007 (2016).
19. H. Chen, H. Li, Y. C. Sun, Y. Wang, and P. J. Lu, "Femtosecond laser for cavity preparation in enamel and dentin: ablation efficiency related factors," *Sci. Rep.* **6**(1), 20950 (2016).
20. T. Petrov, E. Pecheva, A. D. Walmsley, and S. Dimov, "Femtosecond laser ablation of dentin and enamel for fast and more precise dental cavity preparation," *Mater. Sci. Eng., C* **90**, 433–438 (2018).
21. S. Loganathan, S. Santhanakrishnan, R. Bathe, and M. Arunachalam, "FTIR and Raman as a noninvasive probe for predicting the femtosecond laser ablation profile on heterogeneous human teeth," *Journal of the Mechanical Behavior of Biomedical Materials* **115**, 104256 (2021).
22. A. V. Rode, E. G. Gamaly, B. Luther-Davies, B. T. Taylor, J. Dawes, A. Chan, R. M. Lowe, and P. Hannaford, "Subpicosecond laser ablation of dental enamel," *J. Appl. Phys.* **92**(4), 2153–2158 (2002).
23. A. V. Rode, E. G. Gamaly, B. Luther-Davies, B. T. Taylor, M. Graessel, J. M. Dawes, A. Chan, R. M. Lowe, and P. Hannaford, "Precision ablation of dental enamel using a subpicosecond pulsed laser," *Aust. Dent. J.* **48**(4), 233–239 (2003).
24. D. Siniscalco, M. Dutreilh-Colas, Z. Hjezi, J. Cornette, N. El Fels, E. Champion, and C. Damia, "Functionalization of hydroxyapatite ceramics: Raman mapping investigation of silanization," *Ceramics (Basel, Switz.)* **2**(2), 372–384 (2019).
25. H. Tsuda, J. Ruben, and J. Arends, "Raman spectra of human dentin mineral," *Eur J Oral Sci* **104**(2), 123–131 (1996).
26. A. C. T. Ko, L. P. Choo-Smith, M. Hewko, L. Leonardi, M. G. Sowa, C. C. S. Dong, P. Williams, and B. Cleghorn, "Ex vivo detection and characterization of early dental caries by optical coherence tomography and Raman spectroscopy," *J. Biomed. Opt.* (2005).
27. R. Ramakrishnaiah, G. U. Rehman, S. Basavarajappa, A. A. Al Khuraif, B. H. Durgesh, A. S. Khan, and I. U. Rehman, "Applications of Raman spectroscopy in dentistry: analysis of tooth structure," *Appl. Spectrosc. Rev.* **50**(4), 332–350 (2015).
28. L. Zach and G. Cohen, "Pulp response to externally applied heat," *Oral Surg., Oral Med., Oral Pathol.* **19**(4), 515–530 (1965).
29. P. Baldissara, S. Catapano, and R. Scotti, "Clinical and histological evaluation of thermal injury thresholds in human teeth: a preliminary study," *J. Oral Rehabil.* **24**(11), 791–801 (1997).
30. S.-J. Kwon, Y.-J. Park, S.-H. Jun, J.-S. Ahn, I.-B. Lee, B.-H. Cho, H.-H. Son, and D.-G. Seol, "Thermal irritation of teeth during dental treatment procedures," *Restor Dent Endod* **38**(3), 105–112 (2013).

31. K. König and A. Kasenbacher, "Thermal damage behaviour of human dental pulp stem cells" *International Dentistry* 7,2 and *Laser* 4 (2016).
32. D. C. Attrill, R. M. Davies, T. A. King, M. R. Dickinson, and A. S. Blinkhorn, "Thermal effects of the Er:YAG laser on a simulated dental pulp: a quantitative evaluation of the effects of a water spray," *J. Dent. (Oxford, U. K.)* **32**(1), 35–40 (2004).
33. V. L. Lagunov, M. Rybachuk, A. Itthagarun, L. J. Walsh, and R. George, "Modification of dental enamel, dentin by an ultra-fast femtosecond laser irradiation: A systematic review," *Opt. Laser Technol.* **155**, 108439 (2022).